THE JOURNAL OF PHYSICAL CHEMISTRY C

Review Article

Cite This: J. Phys. Chem. C 2017, 121, 26141-26154

pubs.acs.org/JPCC

Probing the Energetics of Molecule−Material Interactions at Interfaces and in Nanopores

Gengnan Li,[†,‡] Hui Sun,[§] Hongwu Xu,*[,∥] Xiaofeng Guo,*[,†,∥,⊥] and Di Wu*[,†,‡,⊥,#]

[†]Alexandra Navrotsky Institute for Experimental Thermodynamics, Washington State University, Pullman, Washington 99163, United States

[‡]The Gene and Linda Voiland School of Chemical Engineering and Bioengineering, Washington State University, Pullman, Washington 99163, United States

[§]Petroleum Processing Research Center, East China University of Science and Technology, Shanghai 200237, China

[∥]Earth and Environmental Sciences Division, Los Alamos National Laboratory, Los Alamos, New Mexico 87545, United States

[⊥]Department of Chemistry, Washington State University, Pullman, Washington 99163, United States

[#]Materials Science and Engineering, Washington State University, Pullman, Washington 99163, United States

ABSTRACT: During the past decades, advances in interfacial chemistries at the molecular level are shaping our world by playing crucial roles in balancing global scale energy crisis and critical environmental concerns. However, systematic investigations into the binding energies, site distribution, and their correlation with the molecular-level surface assemblages and structures at interfaces and in nanopores are rarely documented. In this review, we summarize a set of systematic calorimetric studies on surface energetics we performed during the past decade. These studies demonstrate how thermochemistry can reveal crucial energetic insights into a series of molecule−material interactions relevant to a number of applications, including carbon capture and sequestration, energy production, sustainable chemical processing, catalysis, and nanogeoscience. Calorimetric methodologies developed and applied include direct gas adsorption calorimetry, near-room temperature solvent immersion/solution calorimetry, and high temperature oxide melt solution calorimetry. Using these highly unique techniques, we reveal the thermodynamic complexity of carbon dioxide capture on metal−organic framework (MOF) sorbents with built-in and grafted nucleophilic functional groups (−OH and $-NH_2$). These studies suggest that carbon dioxide adsorption on functionalized MOFs is a complex process involving multiple thermodynamic factors, as reflected by changes in surface phase and structure, chemical bonding, and degree of disorder with varying temperature and gas loading. The fundamental insights obtained may help optimize the design, synthesis, and application of MOF-based carbon dioxide sorbents for carbon capture and sequestration. In parallel, we also explore the energetics of interaction and competition between small molecules (water, carbon dioxide, methane, and simple and complex organics) and inorganic materials (calcite, silica, zirconia, zeolites, mesoporous frameworks, alumina, and uranium), at interfaces and in nanopores. Combined with spectroscopic, diffraction, electron microscopic, and computational techniques, the energetics of gas/liquid−solid interactions can be correlated with specific bonds, molecular configurations, and nanostructures. Although the energetics evolves continuously from weak association to strong bonding to classical capping, distinct regions of rapidly changing stepwise energetics often separate the different regimes. These phenomena are closely related to the properties of inorganic material surfaces (hydrophobicity and acidity/basicity), the framework architectures, and the chemical nature of adsorbate molecules. These direct thermodynamic insights reinforce our understanding of complex small molecule−inorganic material interactions important to multiple disciplines of chemical engineering, materials science, nanogeoscience, and environmental technology, including heterogeneous catalysis, molecular separation, material design and synthesis, biomineralization, contaminant and nutrient transport, carbonate formation, and water−organic competitions on material/mineral surfaces.

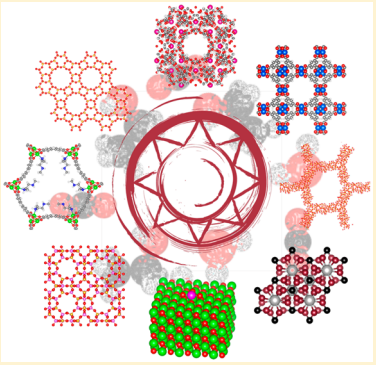

The chemistry of surfaces is of paramount importance in many current technologies, and plays an ever-increasingly vital role in the foreseeable future. The thermodynamics of molecule−material interactions enforces the boundary conditions on many interfacial phenomena that govern the reactivity, selectivity, transformation, and transportation of natural and engineered processes. Example processes include heterogeneous catalysis,[1,2] molecular separation,[3−5] material synthesis[6,7] and modification,[8,9] thermoelectric conversion,[10] environmental transport,[11,12] biomaterials application,[13] and drug delivery.[14,15] Rapid development in material research and chemical industry, and enhanced understanding of earth and

Received: July 27, 2017
Revised: September 27, 2017
Published: October 11, 2017

DOI: 10.1021/acs.jpcc.7b07450
J. Phys. Chem. C 2017, 121, 26141−26154

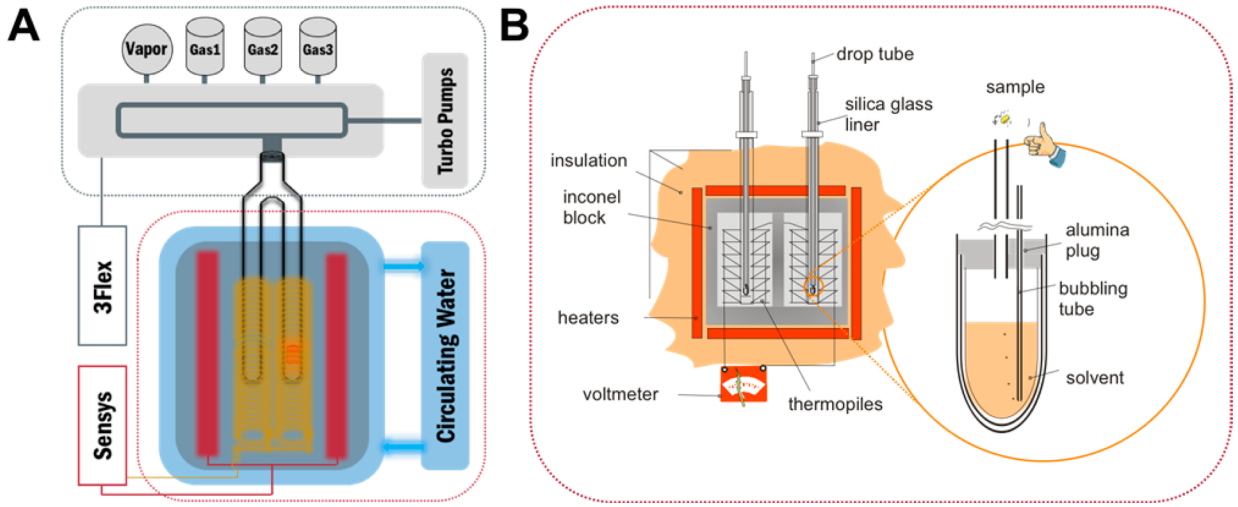

Figure 1. Experimental setups for (A) direct gas/vapor adsorption calorimetry[22,23,37] and (B) high temperature oxide melt solution calorimetry.[16,38]

planetary systems, and biological and medical processes has outrun the existing thermodynamic database, resulting in hindrance for further advancements in these fields. Moreover, the fast development of computational facilities and new computational methodologies at various scales need accurate and reliable thermodynamic data, setting the new benchmark to harness their predictive power. Therefore, there is a rising interest and pressing need for experimentally measured thermodynamic data on molecule−material interactions, namely, adsorption and confinement, to satisfy the overlapping needs in chemistry, materials science and engineering, earth and planetary science, and medical applications. Calorimetry offers a unique yet powerful approach to directly determine such thermodynamic parameters.[16−18]

Earlier thermodynamic studies performed in the Peter A. Rock Thermochemistry Laboratory at UC Davis mainly focused on hydration energetics of nanoparticles (NPs), hydration of zeolites,[19] and organic structural directing agent (OSDA)−framework interactions in zeolite systems.[17,20,21] A full spectrum of experimental thermodynamic (calorimetric) methods have been employed; both homemade and commercially available instruments were used, including water adsorption calorimetry, high temperature oxide melt solution calorimetry, hydrofluoric acid (HF) solution calorimetry, immersion calorimetry, and differential scanning calorimetry (DSC). These techniques enabled accurate surface energy measurements for NPs, and provided the underpinning thermochemical insights into the overall OSDA−framework interactions, which govern the templating and formation of zeolitic phases. It is concluded that both NPs and micro-/mesoporous phases are intrinsically less stable compared with their bulk dense counterparts. Small molecules such as water and OSDA play critical roles in minimizing their excessive surface energies and phase metastability, thereby stabilizing these high surface area and/or open framework materials thermodynamically.[16,17]

In this review, we focus on the recent progress on probing the energetics of molecule−material interactions using experimental thermodynamic (calorimetric) methodologies. Materials (adsorbent or host) studied include metal−organic frameworks (MOFs),[18,22−26] zeolites,[27−30] mesoporous materials,[31−33] nanoparticles,[34] and inorganic oxide heterogeneous catalysts.[35] Molecules (adsorbate or guest) introduced range from water, carbon dioxide, and methane to simple organics, such as ethanol and *n*-hexane. These molecules are commonly seen both in natural environments and under industrial conditions, and play crucial roles in interfacial phenomena encountered in geochemical evolution, and material/chemical processes. Unless otherwise noted, all results presented are experimentally determined using calorimetry.

CALORIMETRY

The word "calorimetry" itself was derived from the Latin word "*calor*" (heat) and the Greek word "*metry*" (to measure).[36] Calorimetry is the science of measurement of heat, which is the energy exchanged within a given time interval in the form of heat flux.[36] Technically, calorimeters are instruments and/or devices designed to perform calorimetric measurements. In the early stage of calorimetric study, because of the extreme difficulty in instrumentation and experimentation, only a few scientists and engineers were able to perform such research.[36] Owing to the advances in electronic and thermal technologies as well as the improved data mining/processing strategies, calorimetry is much more accessible to the general scientific community nowadays. The progress of calorimetric science has been reviewed in detail by Navrotsky.[16,38] Hence, we only briefly introduce those techniques used in the research examples summarized in this review.

Direct Gas or Vapor Adsorption Calorimetry. Direct gas adsorption calorimetry was developed in the Peter A. Rock Thermochemistry Laboratory at UC Davis to study the hydration energetics of inorganic nanoparticles (see Figure 1A).[37] The instrumental system contains a commercial gas adsorption analyzer and a microcalorimeter. In each measurement, about 10−30 mg sample is loaded into one side of a silica glass forked tube, the other side of which remains empty, serving as a reference. Then, the sample is subjected to activation in a vacuum at elevated temperature. During the data collection, the amount of gas adsorbed (adsorption isotherm) and corresponding differential energies of adsorption are simultaneously monitored. Each gas dose leads to a distinct calorimetric peak, which represents the heat generated upon reaching equilibrium for that dose. The differential enthalpies of adsorption can be directly derived using these two sets of data.[22,23,37]

DOI: 10.1021/acs.jpcc.7b07450
J. Phys. Chem. C 2017, 121, 26141−26154

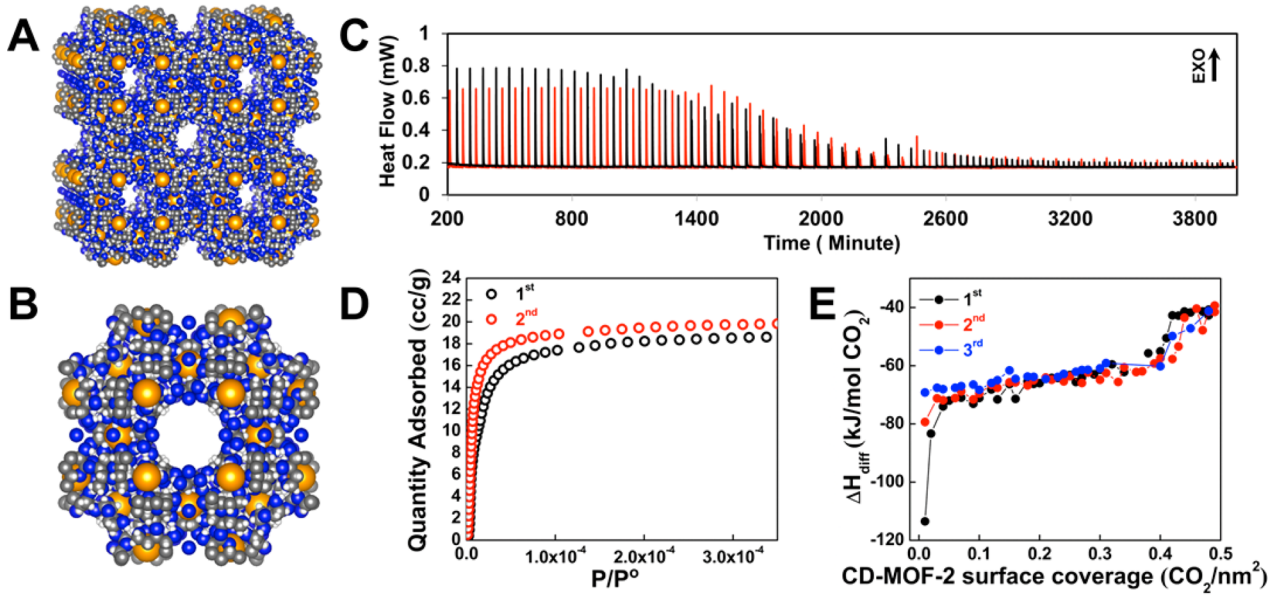

Figure 2. (A) Crystallographic structure of CD-MOF-2 (top). (B) The unit cell containing six γ-CD moieties (bottom). (C and D) The CO_2 adsorption isotherms and corresponding calorimetric traces collected at 25 °C for the first (black) and second (red) adsorption calorimetry on the same sample. (E) Corresponding differential enthalpies of CO_2 adsorption plots.[23]

This versatile technique enables accurate measurement of adsorption enthalpies as a function of gas loading and temperature. Most importantly, the calorimetric data measured are model-independent.[22,23] It is especially powerful when the molecule−material interactions feature (i) strongly exothermic initial adsorption with near-infinite isotherm slopes, (ii) complex, multistep adsorption mechanisms suggesting energetically distinct sites, and (iii) structural or phase evolutions on varying pressure and temperature. In most of these cases, the evolution of adsorption energy may not be accurately derived from direct fitting of adsorption isotherms at different temperatures using the isosteric heat method. We employ the calorimetric technique to investigate the energetics of gas−solid interfacial binding.

High Temperature Oxide Melt Solution Calorimetry. High temperature oxide melt solution calorimetry[16,38] (Figure 1B) is now a major technique for studying the thermodynamic properties of materials, and has diverse applications in the fields of ceramics, nuclear science, mineralogy, geochemistry, etc. Particularly, it is extremely powerful in measuring the enthalpies of formation of ceramic and refectory phases, as the melt solvent kept at high temperature can readily dissolve those types of samples.[16] In our studies on the interfacial interactions, this technique finds its application when the molecular species such as supported metal clusters and super acid moieties form strong covalent or ionic bonds with the material surfaces.

The high temperature oxide melt calorimeter is of twin Calvet-type and has sample chambers maintained at high temperature (>500 °C).[16,38] In a typical experiment, ∼5 mg pellet/chunk of a sample is dropped from room temperature into the chamber. The sharp temperature variance due to dropping, dissolution, and/or reaction is recorded electronically by the thermopiles surrounding the sample chamber and converted to real heat output (enthalpy of drop solution) via a predetermined calibration factor. This measured heat can then be used to derive the enthalpy of formation through appropriate thermochemical cycles. It is worth noting that the high temperature calorimeter can be used to perform multiple thermodynamic measurements, depending on the choice of solvents and experimental atmosphere. Heat content can be measured by transposed temperature drop calorimetry; heats of phase transition and enthalpy of formation can be derived by oxide melt solution calorimetry. Its versatile capabilities have now been applied increasingly to new systems in nanomaterials, catalysts, metallic alloys, high entropy solids, and actinide and transuranium actinide-containing materials.

Near-Room Temperature Solution Calorimetry. The general principle of near-room temperature solution calorimetry is quite similar to that of high temperature oxide melt solution calorimetry. Here, the major difference originates from the solvent selection. Unlike high temperature oxide melt solution calorimetry, which employs molten salts (at high temperature) as solvents, the typical solvent candidates for near-room temperature solution calorimetry are water, aqueous solutions of acid or base, and organics. Additionally, the solvents must be able to completely dissolve the solid sample near room temperature. Further, the measured heats of dissolution are applied to calculate other thermodynamic parameters, such as formation enthalpies and/or molecule−material interactions in OSDA−zeolite[21] or solvent−MOF systems,[27,39,40] etc. Hughes et al. have performed a group of solution calorimetry studies on MOFs.[27,39−41] A series of examples will be given in this review.

Near-Room Temperature Immersion Calorimetry. The enthalpy of immersion is defined as the energetic evolution at constant temperature upon complete immersion of a solid (porous or layered materials or particles) into a liquid or solution, which does not dissolve or react with the bulk body of the solid.[42] In other words, immersion calorimetry aims to measure the interactions at liquid−solid interfaces. Typically, before immersion calorimetry, the solid is completely activated by heating under a vacuum. In other cases, according to the specific research needs, partially or monolayer covered sample with a well-defined initial state can be prepared for the measurement to study the energetic changes at different

DOI: 10.1021/acs.jpcc.7b07450
J. Phys. Chem. C 2017, 121, 26141−26154

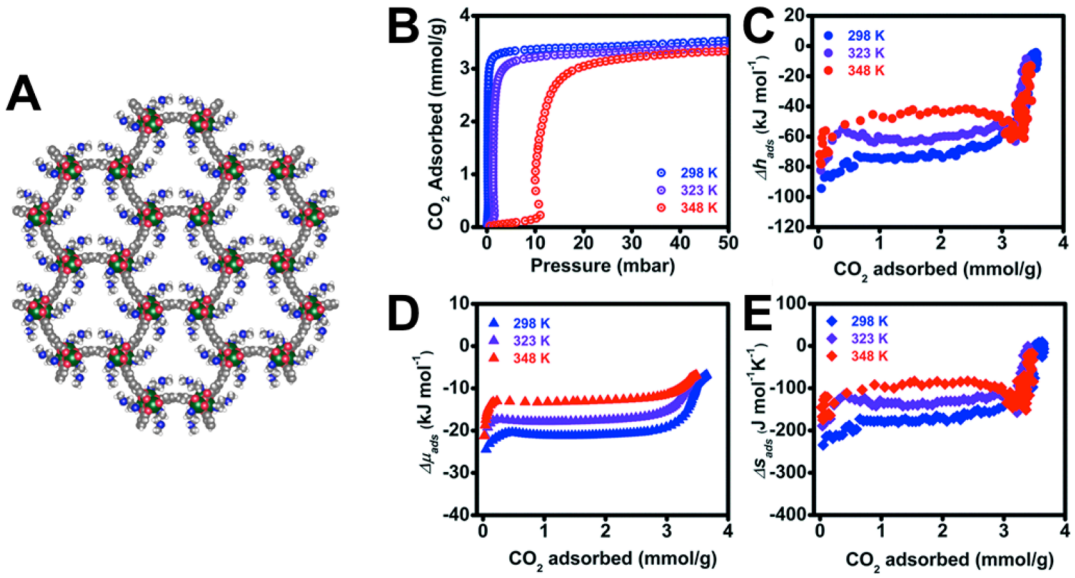

Figure 3. (A) Structure of mmen-Mg_2(dobpdc). (B) CO_2 adsorption isotherms collected at 25 (blue), 50 (purple), and 75 (red) °C. (C) Corresponding differential adsorption enthalpies; (D) differential free energies (chemical potential); and (E) differential entropies of CO_2 adsorption plots.[22]

coverage. Owing to the advantage of direct gas adsorption calorimetry over immersion calorimetry in accurate control of gas/vapor partial pressure, we employ immersion calorimetry only to study the integrated enthalpy change (general energetic effects) due to direct liquid−solid surface interactions.[33]

■ ENERGETICS OF ADSORPTION ON MOFS

MOFs are a group of crystalline porous hybrid solids, which are constructed (assembled) through metal nodes−organic linkers coordination.[43] MOFs have demonstrated superior gas adsorption, storage, and separation capabilities owing to their highly open framework structures, huge surface areas, and the chemical tenability from both metal nodes and organic linkers.[43] In this section, we present a set of systematic studies on the energetics of molecule−MOF interactions and its significance in physical chemistry, catalysis, and material preparation and postsynthesis modification. Examples cover the topics of CO_2 capture, natural gas storage, MOF synthesis, and hydration.

CO_2 Adsorption Calorimetry on MOFs. Four years ago, in collaboration with the Stoddart Mechanostereochemistry Group at Northwestern University, we performed the first, proof-of-principle, adsorption calorimetric measurement to reveal the CO_2 adsorption energetics on an environmentally friendly MOF.[44] The Northwestern researchers synthesized a series of MOF structures from γ-cyclodextrin (γ-CD), a microbiologically derived natural sugar, and naturally abundant alkali metal salts. Additionally, the solvents used in the MOF synthesis are water and alcohols, which are environmentally benign and sustainable.[44,45] Surprisingly, the rubidium (Rb) form, denoted as CD-MOF-2, appears to possess very high CO_2 adsorption selectivity at low pressure and 25 °C. Cross-polarized solid-state nuclear magnetic resonance (NMR) spectroscopic experiments performed by Gessensmith et al.[45] suggest that the hydroxyl groups from the γ-CD building unit, both primary and secondary hydroxyls (see Figure 2), play critical roles in the CO_2−CD-MOF-2 binding, resulting in formation of carbonates.[45] However, the magnitude of CO_2−MOF binding as pressure varies, the binding site map (distribution) in the CD-MOF-2 structure, and the near-zero coverage enthalpy of CO_2 adsorption remain unclear.

The adsorption calorimetric data (Figure 2) measured suggest that the differential enthalpy of CO_2 adsorption is stepwise as pressure increases from high vacuum.[23] First, an irreversible chemisorption involving merely a small number of sites is observed at near-zero coverage. These strongly exothermic binding events, starting from −113.5 ± 0.9 kJ/mol CO_2, likely on the most reactive primary hydroxyl groups, are followed by the less strong, reversible, major chemisorption (−65.4 ± 1.6 kJ/mol CO_2). The binding with intermediate strength forms the first plateau in the differential enthalpy of adsorption plot, spanning from 0 to 0.4 CO_2/nm^2 (see Figure 2). This plateau in energy represents the CO_2 adsorption on the less reactive, vast majority of hydroxyls. Eventually, the sorption is concluded at the second plateau at −40.0 ± 1.8 kJ/mol CO_2—clear evidence showing much weaker physisorption between CO_2 and CD-MOF-2. Therefore, this study confirms the presence of at least two energetically distinct sites for CO_2 chemisorption on CD-MOF-2. Meanwhile, this work also demonstrates that direct gas adsorption calorimetry is a powerful tool for determining adsorption energetics for systems that feature strong initial sorption and multistep reaction stages.[23]

Once the metal nodes of MOF are coordinatively unsaturated, they can be further functionalized by grafting molecular species with nucleophilic groups, resulting in additional functional materials for adsorption, catalysis, and separation. We collaborated with the Long Group at UC Berkeley to study the thermodynamics of CO_2 adsorption on a diamine-functionalized Mg-MOF-74 analogue, mmen-Mg_2(dobpdc).[17] This diamine-grafted MOF has demonstrated an intricate "phase-transition-like", cooperative insertion CO_2 adsorption mechanism near room temperature.[46] To further investigate the energetic evolution of CO_2 adsorption on mmen-Mg_2(dobpdc) as temperature varies, we carried out calorimetric measurements not only at 25 but also at 50 and 75 °C (see Figure 3).[17] The results revealed a detailed dependence of adsorption enthalpy, entropy, and free energy as a function

DOI: 10.1021/acs.jpcc.7b07450
J. Phys. Chem. C 2017, 121, 26141−26154

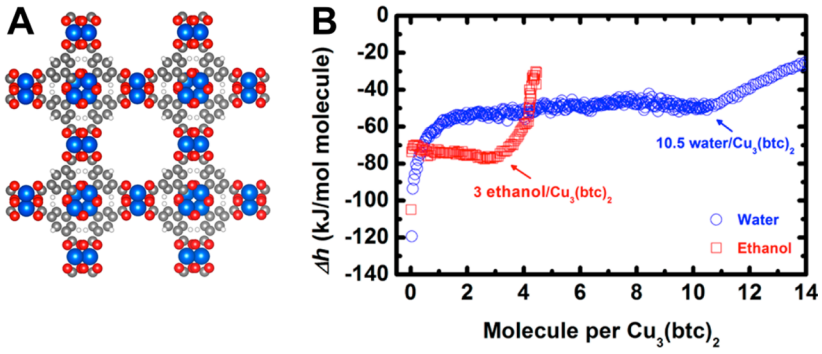

Figure 4. (A) The copper HKUST-1 structure. (B) Differential adsorption enthalpy curves for water (blue) and ethanol (red) versus the number of moles of molecules adsorbed per mole of $Cu_3(btc)_2$.[26]

of pressure and temperature. First, the calorimetric data indicate the potential presence of three types of binding. The strongest sorption takes place at a very low loading, which is −94.4 ± 2.8 kJ/mol CO_2. The major chemisorption at intermediate loadings is moderately exothermic (−75 ± 2.2 kJ/mol CO_2), which is primarily due to the CO_2−amine cooperative insertion mechanism. The least exothermic physisorption events appear when all of the amine groups are saturated as ∼3 mmol of CO_2 are adsorbed on 1 g of sorbent.

Further, we derived the partial molar properties for the CO_2−mmen-Mg_2(dobpdc) system based on the adsorption isotherms (intrinsically a chemical potential curve) and enthalpy data.[17] Interestingly, analysis suggests that the differential adsorption enthalpy, entropy, and chemical potential all become less negative as temperature increases (Figure 3). These thermodynamic evidences all suggest increased adsorbent surface entropy at higher temperatures, which presumably indicate enhanced surface dynamics/motion at the molecular levels. Indeed, such phenomena correspond well with weaker CO_2−mmen-Mg_2(dobpdc) interactions at elevated temperatures.

The outcome of these two examples lays the foundation for further exploration of the energetics of adsorption and confinement effects of molecules on MOFs. These studies also highlight the thermodynamic complexity of CO_2 adsorption on functionalized MOFs, especially the interplay between energetic and entropic factors, and their tight relation with the surface structure, molecule−material bonding, and degree of order/disorder as pressure and temperature evolve. In a broader sense, the fundamental thermodynamic insights into molecule−MOF binding may aid material scientists to design and tune new MOF-based sorbents, which may be applied in the chemical industrial processes, in which the energetics of surface reactions are vastly important.

Methane Storage in MOF on Cu-HKUST-1 at Low Pressure. Other than strong chemisorption, direct gas adsorption calorimetry is also very sensitive to weak binding at low pressure, such as methane (CH_4). Owing to their unique tunable surfaces and structures, MOFs can be designed and constructed to serve as methane storage materials. Utilizing adsorption calorimetry, we studied the thermodynamics of CH_4 adsorption on Cu-HKUST-1 at 25 °C at pressures below 1 bar.[25] In such a low-pressure range, the methane intermolecular interactions are minimized. In other words, the differential adsorption energies measured solely represent the direct interactions between CH_4 and the framework. The calorimetric results show that the differential CH_4 adsorption enthalpy is constant in the low-pressure range investigated in this work. Moreover, it appears that the CH_4−MOF interaction tends to be more sensitive to the dimension of the smallest accessible MOF pore or channel than to the polarizability of the guest molecule and the Cu sites. An identical conclusion was reached in a separate study by Hulvey et al., in which neutron powder diffraction experiments and periodic density functional theory (DFT) calculations were carried out.[47] In short, the calorimetric results are in excellent agreement with those of crystallographic and theoretical studies, which all suggest that, in initial, low pressure adsorption, the CH_4−HKUST-1 interaction tends to be more sensitive to the confinement effects from MOF structures, indicating a less significant role for the Cu node.

Solvent−Framework Interactions in MOF Synthesis. The solvent−MOF interactions are chemically complex.[48] The materials we studied may be roughly categorized into two types based on the degree of coordination of the MOF metal nodes. For MOFs with saturated metal nodes (no clearly defined binding sites), the solvent molecules merely act as "space-fillers". Consequently, upon solvent removal, the crystalline MOF structures typically persist without structural degradation. In contrast, for some MOF structures, the metal sites are not saturated by the organic linker coordination. Instead, they bind solvent molecule so strongly through chemisorption that solvent removal would lead to eventual structural collapse. The solvent−MOF interactions were also discussed in an earlier solution calorimetry study of the formation energetics of paddle wheel MOFs.[27]

In this regard, we employed solution calorimetry to study the thermodynamic effects of solvents on MOF-5 synthesis and formation.[24] The solution chosen for our calorimetric measurement was NaOH (5 M at 25 °C), in which the sample was completely dissolved, and the dissolution enthalpies (ΔH_{ds}) were obtained. Subsequently, we used the ΔH_{ds} values to calculate the enthalpies of formation (ΔH_f) of MOF-5·DMF and MOF-5·0.60DEF from their corresponding dense phase assemblages, zinc oxide (ZnO), 1,4-benzenedicarboxylic acid (H_2BDC), *N*,*N*-dimethylformamide (DMF), and *N*,*N*-diethylformamide (DEF). The results show that the formation enthalpy of MOF-5·DMF is 16.69 ± 1.21 kJ/mol Zn_4O, while the MOF-5·0.60DEF formation results in an endothermic heat effect of 45.90 ± 1.46 kJ/mol Zn_4O. Applying the formation enthalpy of solvent-free MOF-5 measured earlier, the interaction enthalpies (ΔH_{int}) for DMF−MOF-5 and DEF−MOF-5 interactions were calculated to be −82.78 ± 4.84 kJ/mol DMF and −89.28 ± 3.05 kJ/mol DEF, respectively. These

DOI: 10.1021/acs.jpcc.7b07450
J. Phys. Chem. C 2017, 121, 26141−26154

strongly exothermic enthalpies of interaction values suggest that the solvents (Lewis bases) tend to bind more strongly with the electron accepting Zn_4O nodes at low coverage than at high solvent loading, as seen in the study of Hughes et al.[40] In other words, the enthalpies of solvent−MOF interactions are mostly governed by the electron accepting−donating processes, rather than the pore filling mechanisms. The calorimetric results shown here provide useful energetic insights, which may benefit MOF synthesis and postsynthesis modification, such as transmetalation and solvent assisted linker exchange (SALE).[48]

Hydration Energetics of Paddle-Wheel MOF Cu-HKUST-1. The hydration enthalpy on copper HKUST-1 was investigated directly using water adsorption calorimetry.[26] Due to its structural complexity (three pore sizes and the presence of copper site), the hydration process of Cu HKUST-1 is also complicated. Specifically, the strongest near-zero coverage water−MOF binding is −119.4 ± 0.5 kJ/mol water in energy. We suspect it perhaps represents water confinement in the smallest (4 Å) cages. Further evidence from spectroscopy or diffraction data is needed to verify this hypothesis. Subsequently, the differential enthalpy of water adsorption becomes less exothermic and levels at the first plateau at −50.2 ± 1.8 kJ/mol water. The position of this plateau is in excellent agreement with the results from the solution calorimetry study performed by Bhunia et al.,[27] which corresponds to the coordination between water and the open Cu nodes, and subsequent filling of the largest (11 Å) pores.[27] Later, the differential enthalpy trace ramps up to its second plateau, indicating the weakest interactions on the hydrophobic MOF surface. Furthermore, combining ethanol adsorption calorimetry (see Figure 4), mathematical slope analysis of the water adsorption isotherm, and the differential enthalpy of hydration trace, we attempted to develop a method to achieve quantitative separation of a series of energetically similar binding events. These results and interpretation are promising, yet we do need support from spectroscopic, crystallographic, and computational methodologies to reach a definite conclusion.[26]

CONFINEMENT ENERGETICS IN INORGANIC POROUS MATRIXES

Nanoconfinement of molecular species, the guest−host interactions in micro- and mesoporosity, lays the foundation for heterogeneous catalysis, geochemistry, nanomineralogy, and nanomedicine. In this section, we summarize our recent studies on the energetics, structure, and dynamics of molecules upon confinement in nanoscale or sub-nanoscale pores of inorganic matrixes. We started with the "trilogy" on ion-exchanged zeolite A,[28−30] in which the hydration and formation energetics[29,30] and thermodynamics of *n*-hexane confinement were explored and discussed.[28] We then explored the guest−host interactions in mesoporous materials, including pure silica MCM-41 and SBA-15.[32,33] More specifically, a series of mesoporous silicas with various pore/channel dimensions (0.8−20.0 nm) were synthesized to accommodate a spherical, rigid, organic molecule, *N*,*N*,*N*-trimethyl-1-adamantammonium iodide (TMAAI). We carefully examined the magnitude of interaction energetics and analyzed the structural and dynamic (motion) evolution of guest species upon confinement in pores/channels of different dimensions. The most significant outcome was that we generalized a conceptual model with three types of guest species inclusions versus the relative size of host pores and guest objects. They are single-molecule confinement, multi-molecule adsorption/confinement, and nanocrystal confinement. Lastly, we evaluated the crucial role of hydroxyl concentration on molecule−silica surface interactions.[49]

Energetics and Hydration of Ca−Na Ion-Exchanged Zeolite A. Intrinsically, hydration of zeolites is indeed the confinement of water in the void space of the zeolitic frameworks. Unlike other simple binary guest−host systems, introduction of charge-balancing cations has brought additional complexity in both structure and energetics. To study the hydration and thermodynamics of ion-exchanged zeolites, we prepared a series of Na−Ca exchanged zeolite A samples with various Ca contents, ranging from 0 to 97.9%.[29] They were fully characterized using powder X-ray diffraction (XRD), thermogravimetric analysis (TGA), and differential scanning calorimetry (DSC). We utilized high temperature oxide melt drop solution calorimetry to quantify the enthalpies of formation for hydrated zeolites CaNa-A from their constituent oxides. Specifically, the formation enthalpies of zeolites CaNa-A are shown to have a linear dependence as the degree of Ca exchange increases. The enthalpy of formation from the oxides at 25 °C becomes less exothermic as more Na^+ cations are substituted by Ca^{2+}, from −74.50 ± 1.21 kJ/mol TO_2 (T represents atoms on the tetrahedrally coordinated sites) for hydrated Na-A to −30.79 ± 1.64 kJ/mol TO_2 for hydrated 97.9% CaNa-A (Figure 5).

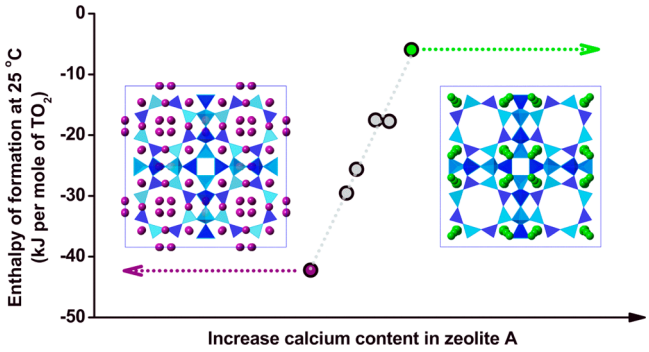

Figure 5. Structures of sodium (left) and calcium (right) ion-exchanged zeolite A and formation enthalpies of hydrated sodium and calcium ion-exchanged zeolite A from oxides as a function of average ionic potential.[29]

Meanwhile, the water content of zeolites CaNa-A appears to increase linearly as the degree of Ca^{2+} exchange increases, from 20.54% for Na-A to 23.77% for 97.9% CaNa-A, while the corresponding enthalpies of dehydration (from DSC analysis) monotonically decrease, from 32.0 kJ/mol H_2O for Na-A to 20.5 kJ/mol H_2O for 97.9% CaNa-A. Indeed, the substitution of Na^+ by Ca^{2+} increases the average ionic potential of charge-balancing cations (Na^+ and Ca^{2+}) and results in less exothermic formation enthalpies, an indication of less stable zeolitic frameworks, which has similar energetic effects as stabilizing through hydration.[29]

Further, we expanded our study to all alkali and alkaline earth ion-exchanged zeolites A (see Figure 6).[30] Their enthalpies of hydration and formation from constituent oxides were experimentally measured by TG-DSC and high temperature oxide melt solution calorimetry. Similarly, the calorimetric insights suggest that zeolite A has a linearly increased hydration level with less negative formation enthalpies as the average ionic potential of guest cation increases. Particularly, the level of hydration for zeolite A increases linearly as the average ionic potential (Z/r) of the cation increases, from 0.894 for Rb-A to

DOI: 10.1021/acs.jpcc.7b07450
J. Phys. Chem. C 2017, 121, 26141−26154

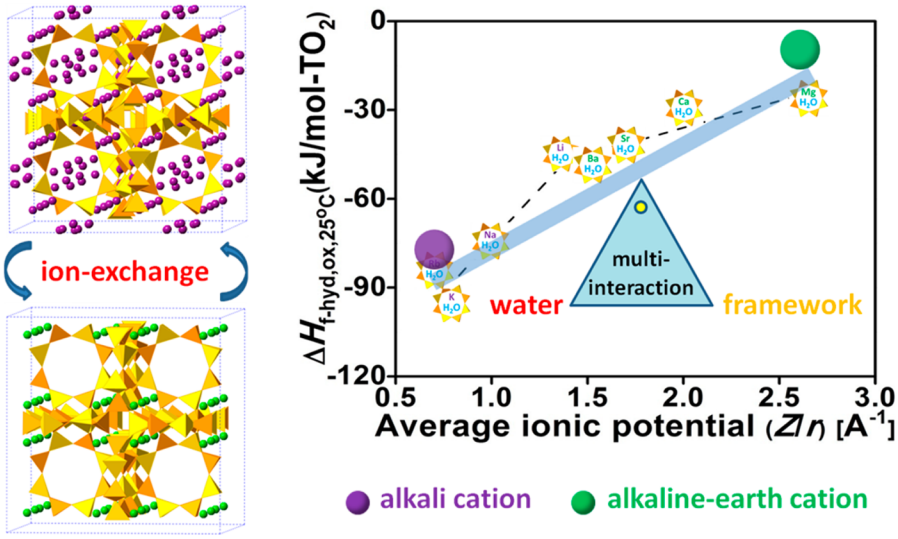

Figure 6. Structures of alkali (left top) and alkaline earth (left bottom) ion-exchanged zeolite A and formation enthalpies of hydrated alkali and alkaline earth ion-exchanged zeolite A from oxides as a function of average ionic potential.[30]

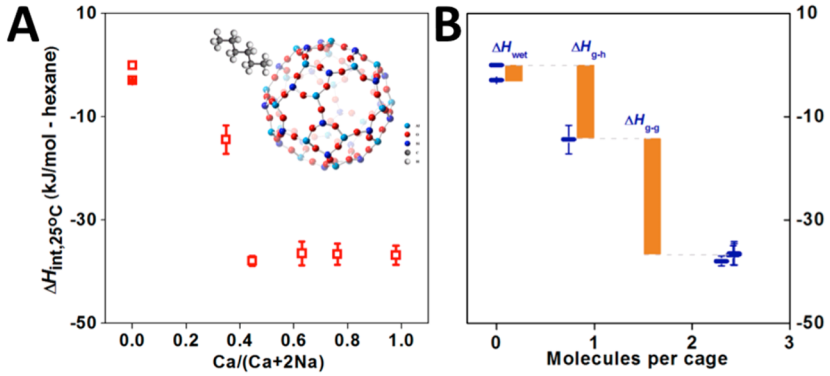

Figure 7. (A) Enthalpies of interactions upon *n*-hexane confinement in zeolite NaCa-A. (B) Energetic contributions from different factors for *n*-hexane−zeolite A interactions.[28]

1.317 water per TO_2 for Mg-A. Meanwhile, the enthalpies of formation from constituent oxides at 25 °C range from −93.71 ± 1.77 for K-A to −48.02 ± 1.85 kJ/mol per TO_2 for Li-A for hydrated alkali zeolite A and from −47.99 ± 1.20 for Ba-A to −26.41 ± 1.71 kJ/mol per TO_2 for Mg-A for hydrated alkaline earth zeolite A. Interestingly, distinctly different slopes were seen between the alkali and alkaline earth zeolite A.[30]

These two studies strongly suggest that the hydration generally stabilizes zeolites yet the hydration energetics is complex, the exact trend of which largely depends on the water−cation−framework interplays.[29,30]

Confinement of *n*-Hexane in Ca−Na Ion-Exchanged Zeolite A: Cation Is the "Goalkeeper". Understanding the thermodynamics of confinement of organic molecules in sub-nanoporosity and nanoporosity forms the foundation for material synthesis, catalysis, adsorption, and separation. As demonstrated above, the type of cations and degree of ion-exchange are critical factors governing the crystallinity and energetic stability of zeolites. Other than significantly modifying the formation and hydration energetics, the pore accessibility for zeolite A can also be tuned by ion-exchange. To be exact, for the LTA structure, the aperture of pure zeolite Na-A is 3.8 Å, while it becomes 4.3 Å once all monovalent sodium cations are exchanged by the divalent Ca^{2+} (see Figure 5). Such angstrom scale tuning leads to inaccessible, partially accessible, and fully accessible central cavities (alpha cage) to guest species, such as water and *n*-hexane. On this topic, we collaborated with the Sun Group at East China University of Science and Technology (ECUST) in China to explore the energetics of guest−host interactions in zeolites.[28] We started with the confinement thermodynamics of *n*-hexane in Na−Ca exchanged zeolite A samples with different degrees of Ca^{2+} exchange. Combining immersion calorimetry and thermogravimetric analysis coupled with mass spectroscopy (TGA-MS), we were able to obtain the interaction enthalpy trend for the *n*-hexane−Na−Ca exchanged zeolite A system. Specifically, as the Ca^{2+} content increases from 0 to nearly 100%, the enthalpy of *n*-hexane−zeolite A interactions tends to be more exothermic until reaching a plateau at about −40 kJ/mol *n*-hexane (Figure 7A). Moreover, we attempted to interpret and separate the contributions from various types of interactions to the overall confinement (Figure 7B). To be exact, the external surface wetting accounts for −2.9 kJ/mol *n*-hexane, while the zeolitic framework contributes −14.4 kJ/mol *n*-hexane to the overall interaction energy. Surprisingly, the *n*-hexane intermolecular interactions in the zeolite framework exhibit the most exothermic heat effect of −22.2 kJ/mol *n*-hexane. Thus, to study the confinement energetics, the guest−guest intermolecular interactions must be considered.[28]

DOI: 10.1021/acs.jpcc.7b07450
J. Phys. Chem. C 2017, 121, 26141−26154

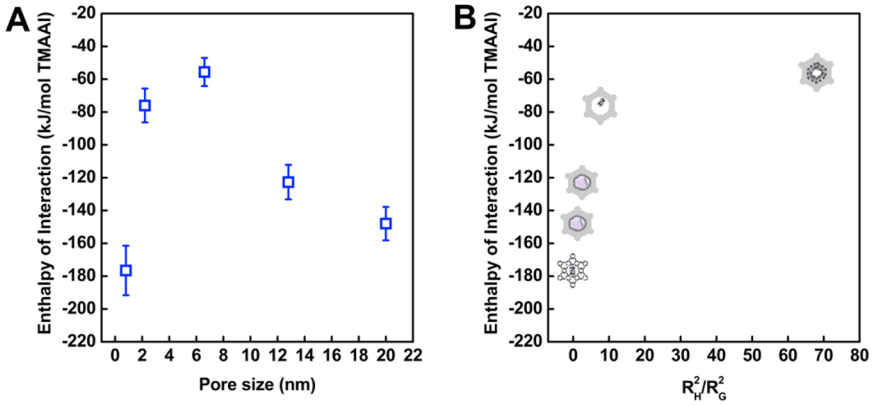

Figure 8. (A) Interaction enthalpies for porous silica samples per mole of TMAAI as a function of framework pore size. (B) Interaction enthalpies for porous silica samples per mole of TMAAI vs (pore size/guest size)^2 [32]

Small Molecule−Silica Interactions in Porous Silica Matrixes: Interplay of Confinement and Adsorption. Confinement of molecules in nanoporosity is more complex due to the introduction of guest−guest interactions, the much more open pore/channel structures, and the tunable material surfaces, both internal and external. In an earlier study emphasizing the geological behaviors of porous silicas in CO_2 sequestration environments, our immersion calorimetry results suggest that the energetics of small molecule−porous silica interactions are determined by both framework pore dimension and concentration of its surface groups (hydroxyls).[33] Additionally, it appears that the relatively hydrophobic silica surface favors small organic molecules, such as alcohol and amines, more than aqueous solutions, including pure water and NaCl brine.[33] In other words, the overall energetic trend suggests that silica with smaller pores/channels and higher hydroxyl concentration may lead to stronger molecule−material interactions. Moreover, the calorimetric results indicate that organics tend to coat onto the silica surfaces, while water or aqueous solutions appear to form clusters, which are higher in energy than that of bulk water, "floating" on top of the relatively hydrophobic surface of silica.[33] This work has generated many interesting questions and topics, which directly lead to our subsequent studies on the two model systems on confinement and adsorption, described below.

As stated earlier, the molecular-level organic−inorganic interactions in framework materials are critical in understanding many phenomena in catalysis, material modification, nanomedicine, and nanogeoscience involving confinement of organics in nanoscale porosity. To reveal the energetic insights into the complex interactions between organic molecular guest and inorganic framework host, especially the confinement effects as pore/channel dimension evolves, we engineered a model system containing a spherical, rigid, organic molecule, *N*,*N*,*N*-trimethyl-1-adamantammonium iodide (TMAAI), and a series of porous silica frameworks (one zeolite and a few mesoporous silicas) with different void dimensions from 0.8 to 20.0 nm.[32] Technically, hydrofluoric acid (HF) solution calorimetry was employed to directly measure the overall guest−host interaction enthalpies. We found out that the enthalpies of TMAAI−silica interactions range from −56 to −177 kJ/mol TMAAI. Interestingly, the enthalpy of interactions shows an exponential dependence on the relative size of host dimension and guest species (see Figure 8). Combining the calorimetric results with data obtained from XRD, IR, TG-DSC, and solid-state NMR, we were able to determine the enthalpies of interaction between TMAAI and the porous silica frameworks, to identify and interpret the assemblage, phase, and dynamics of confined guest molecules, and to distinguish different types of guest−host interactions. They are single-molecule confinement in angstrom scale microporosity, multi-molecule adsorption/confinement of a disordered and presumably highly dynamic (mobile) assemblage of guest species near the pore/channel walls, and nanocrystal confinement at the center of the pore/channel.[32] In a thermodynamic sense, such structural evolution upon confinement probably reflects matched specific structure, motion dynamics, and minimized overall free energy for the entire guest−host system.[32]

Surface Binding: The Crucial Role of Concentration of Functional Group. To better our fundamental knowledge on silica surface chemistry, which is essential for its applications in surface sciences and engineering, we used direct gas adsorption calorimetry at 25 °C to study the adsorption energetics of water and ethanol on a silica glass, CPG-10 in both hydroxylated and dehydroxylated forms.[49] CPG-10 was chosen as the silica candidate because it did not show detectable structural degradation upon calcination for complete dehydroxylation at 800 °C. The calorimetric data reveal complex adsorption energetics as a function of pressure (coverage). Interestingly, ethanol exhibits a stepwise differential enthalpy of adsorption profile, whereas the sorption energetics for water appears to be largely continuous. Particularly, at near-zero coverage, the adsorption enthalpies on the hydroxylated silica surface are the most exothermic. For water and ethanol, they are −72.7 ± 3.1 and −78.0 ± 1.9 kJ/mol molecule, respectively. In other words, the initial binding of both molecules on the silica surface defects has nearly identical magnitude in energy. As pressure increases, the enthalpy trace of water adsorption tends to be less exothermic, which gradually reaches its only plateau at −20.7 ± 2.2 kJ/mol water. This value is more than 50% less exothermic than that of water condensation (−44.0 kJ/mol water), clear evidence suggesting formation of water clusters on a largely hydrophobic surface.[49] In sharp contrast, the ethanol adsorption enthalpy curve appears to have two distinct plateaus at −66.4 ± 4.8 and −4.0 ± 1.6 kJ/mol ethanol, which are indicative of strong chemisorption on adsorbate-free and weak physisorption on ethanol monolayer coated silica surfaces, respectively.[49] Moreover, we also found out that dehydroxylation results in the absence of water−silica interactions, whereas ethanol does not show significantly selective binding onto the silanols and the hydrophobic areas of the silica

DOI: 10.1021/acs.jpcc.7b07450
J. Phys. Chem. C 2017, 121, 26141−26154

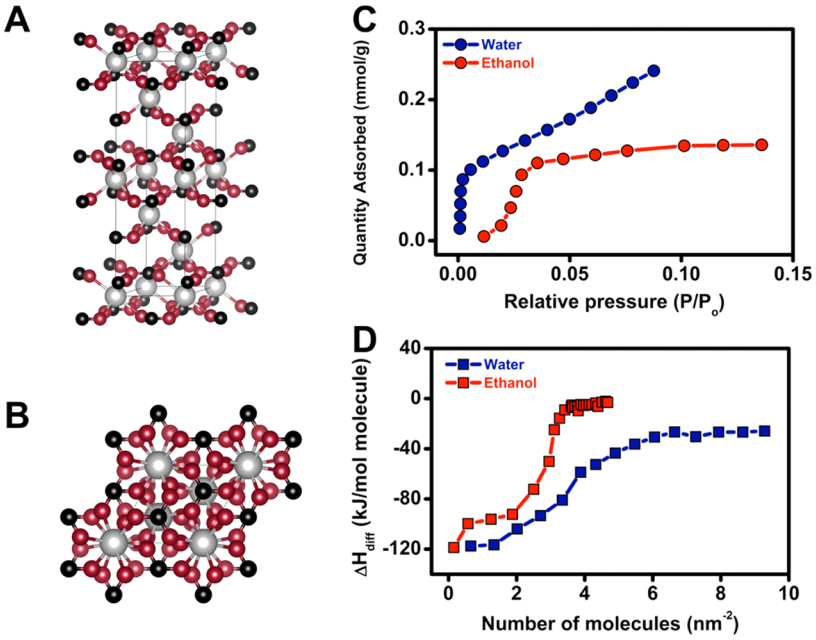

Figure 9. (A) Calcite structure. (B) Calicite {0001}. (C) Water and ethanol adsorption isotherms. (D) Corresponding differential enthalpies of adsorption for a nanocalcite sample denoted as NMT-2 at 25 °C.[34]

surface.[49] These very fundamental thermodynamic data form the basis for the physical chemistry of surfaces, and need to be seriously considered by the scientific and engineering communities.

■ ENERGETICS OF ORGANIC–NANOPARTICLE INTERACTIONS

Thermodynamics of Ethanol–Nanocalcite Interfacial Interactions. Understanding the energetics of organic–nanoparticle (NP) binding is critical to harnessing the reactions encountered in industrial applications and to understanding various geochemical reactions, such as aerosol formation and biomineralization. In our study on the energetics of organic–NP interactions as a function of molecular coverage, we selected the ethanol–nanocalcite system for the direct adsorption calorimetric measurements with an aim of mimicking the organic–NP binding in various systems and under different conditions.[34] We found the interactions were energetically stepwise yet chemically continuous, evolving from molecule (ligand) capping to strong bonding to weak association as the adsorbate coverage varies (see Figure 9). Specifically, the ethanol adsorption energetics on calcite nanocrystals at room temperature is complex with a series of binding events as its coverage increases. The most exothermic sorption was observed on the fresh, near-zero coverage nanocalcite surfaces, which is typically seen for adsorption on a NP surface with intrinsic defects. The strongest binding is followed by the major chemisorption prior to ethanol monolayer formation, exhibiting a plateau which levels at about −98.3 ± 4.8 kJ/mol ethanol. Finally, the adsorption calorimetric data is concluded with the least exothermic, near-zero-magnitude, physisorption (second differential enthalpy of adsorption plateau).[34]

The strong adsorption energetics suggests a unique surface structure, as predicted by molecular dynamics and DFT calculations.[50] Specifically, in the ethanol monolayer formation, the polar end of ethanol (hydroxyl group) is tightly bonded to the calcite nanocrystal surface through strong hydrogen bonding. This leaves the hydrophobic tails of the ethanol molecules facing outward, interacting merely weakly with the ethanol vapor. As a result, an angstrom scale low ethanol density, spatial gap between the monolayer and subsequent molecules was formed. Indeed, such subtle variations in surface assemblages can have significant effects on the reactivity, selectivity, and stability of NP surfaces, which may impact surface reactions as well as the self-assembly of molecular species and nucleation and growth of nanocrystals on and around organic-capped surfaces. In a much broader sense, the thermodynamic fundamentals revealed in the ethanol–calcite system may enhance our understanding on similar phenomena encountered in natural environments and chemical industrial processes.

■ CATALYST SYNTHESIS AND STABILITY

Thermodynamic Complexity of Sulfated Zirconia Catalysts. Understanding the energetics of bonding (interactions) between molecular-level catalytically active species and catalyst support is essential for catalyst synthesis, optimization, and stability. A systematic study was performed on the thermodynamics of sulfated zirconia catalysts, in which two critical topics regarding catalyst synthesis and surface energetics were investigated.[35] They are sulfuric acid immersion (catalyst precursor preparation) and sulfate–zirconia interfacial bonding. First, we synthesized a series of sulfated zirconia (SZ) catalysts by immersion of amorphous zirconium hydroxide in sulfuric acid of different concentrations (C). They were characterized using XRD, TGA-MS, sulfuric acid immersion calorimetry, and high temperature oxide melt solution calorimetry. We directly measured the enthalpies of sulfur species–zirconia surface interactions (ΔH_{SZ}) using sulfuric acid immersion calorimetry, which range from −109.46 ± 7.33 (1 N) to −42.50 ± 0.89 (4 N) kJ/mol S. These ΔH_{SZ} values display a roughly exponential trend, more exothermic linearly as sulfur coverage increases. We needed to use high temperature oxide melt drop solution

DOI: 10.1021/acs.jpcc.7b07450
J. Phys. Chem. C 2017, 121, 26141−26154

calorimetry to study the SZ formation, since the bonding between sulfur species and zirconia surfaces is primarily covalent. The formation enthalpies of SZ (ΔH_f) appear to be more exothermic linearly, from -147.90 ± 4.16 (at 2.1 nm^{-2}) to -317.03 ± 4.20 (at 2.3 nm^{-2}) kJ/mol S, as sulfur surface coverage increases (Figure 10). This implies formation of

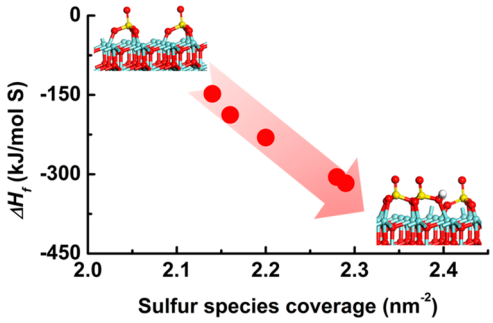

Figure 10. Formation enthalpy of sulfated zirconia from constituent oxides for sulfated zirconia made at 650 °C as the sulfur species surface coverage varies. The structural illustrations are monosulfate (left) and polysulfate (right).[35]

energetically more stable polysulfate species as seen in other noncalorimetric studies. Indeed, the thermodynamic insights obtained here are tightly correlated to the configuration of sulfur species, which is a function of surface coverage. In a slightly broader sense, studying the thermodynamics of catalyst synthesis and the active species−support interaction energetics may compliment the existing spectroscopic and structural characterization techniques, thereby enhancing our understanding on the stability and activity of solid state catalysts.[35]

Very recently, we studied the energetic expense of transition metal doping on mesoporous γ-Al_2O_3 using density functional theory (DFT).[51] The results suggest that the aluminum vacancy (V_{Al}) concentration decreases with increasing atomic number of the transition metal dopant, due to charge compensation effects. The topic of molecule−material interactions on this set of phases is of great interest, and is currently being investigated using calorimetric methods.

■ CONCLUDING REMARKS AND PERSPECTIVES

Recent development of materials synthesis enables systematic design and construction of nanostructured material surfaces and framework structures to facilitate controllable functionality for energy conversion, carbon capture, catalysis, self-assembly, molecular recognition, and biomedical diagnosis. Despite the dramatic variations in physical and chemical properties, the commonality of these material surfaces is that they are heterogeneous with structural sites of distinct energetic states. In this review, we have demonstrated that such energetic heterogeneity can be accurately probed and separated using calorimetric methods. The general observation is that, although the energetics appears to be stepwise, the evolutions from weak attachment to strong binding to classical capping are a series of continuous events, forming a downward energetic landscape. Indeed, such phenomena are governed not only by the nature of material surfaces and framework structures but also by the guest−guest or adsorbate−adsorbate interactions. The competitions and interplay among these factors are of great complexity, yet one can employ calorimetric techniques to quest for the energetic insights into the molecule−material interactions at their interfaces and/or in nanopores.

In our ongoing and future exploration, the energetics of molecule−material interactions relevant to biomass conversion, CO hydrogenation and oxidation, methane steam reforming and activation, transition metal doping in oxides, electrochemical and photochemical processes, and molecular sensing will be studied thoroughly. For the catalytic materials involved in these processes, the variation, distribution, and concentration of surface active components or sites may induce substantial changes in the chemical nature for surface reactions. In contrast to our traditional understanding, under certain circumstances, especially the operating conditions at elevated temperature and pressure, the nature of the nanomaterial surface is dynamic and evolving. Along this line, we will center on gaining insights into both the chemical and thermodynamic bases for molecule−material interactions at or near their interfaces, with particular emphasis on the direct calorimetric measurements of binding enthalpies and site distribution simultaneously. Combined with *in situ* structural characterization and multiscale computational simulations, we will probe the surface heterogeneity and their evolution before, during, and after the reactions, with an emphasis on the reaction mechanisms and associated thermodynamics/kinetics. More specifically, the short-range order of local binding will be explored by NMR and X-ray or neutron pair distribution function (PDF) analysis, while medium- and long-range structural order will be examined by various synchrotron-based X-ray scattering techniques. Additionally, electron microscopy, such as scanning electron microscope (SEM), transmission electron microscope (TEM), and atomic force microscopy (AFM), will be used to characterize the nanostructure and morphology. By tracking the evolution of specific chemical bonding, molecular configuration, nanostructure, and energetics of molecule−surface interactions, the heterogeneity and dynamics of surfaces, the reaction mechanisms, as well as the underlying chemistry−function relations can be systematically studied.

Besides the typical geochemical significance of molecule−material interfacial binding, knowledge of interactions between actinide-containing phases with small molecules (H_2O, CO_2, small organics, etc.) is pivotal for understanding the underlying processes when actinides enter the environment. This includes the adsorption/desorption of molecules at their interfaces with actinide solids and the complex surface reactions involving various molecular species and actinide-bearing phases. Water molecules, for instance, may participate in many stages of actinide surface reactions. Here we list a few representative examples. As a catalyst, water can facilitate the oxidation of U(IV) and P(IV) binary oxides where solely molecular oxygen cannot oxidize PuO_2.[31,52−55] Additionally, the corrosion effects of water on actinides are substantial.[55−57] Compared with dry air, the corrosive rate of plutonium substantially increases when exposed to moisture.[56,58] The surface reactions of spent nuclear fuels or high-level wastes with water could also thermodynamically lead to degradation or phase alteration, in the form of coffinite,[59−61] peroxides (studtite, metastudtite),[62−65] metaschoepite, nanoscale complexes/clusters,[66,67] etc. These reactions at the micro- or mesoscopic scales could widely occur in a geological repository of storing spent fuel and nuclear waste, and a nuclear plant accident, such as Fukushima Daiichi nuclear disaster.[68]

Moreover, actinide species can exist in the forms of small clusters or colloids, which can have significant interactions in a

DOI: 10.1021/acs.jpcc.7b07450
J. Phys. Chem. C 2017, 121, 26141−26154

variety of ways with solid phases under certain environmental settings. In our opinion, studies on small actinide species not only contribute to the understanding of the first stage reactions (crystallization, sorption, etc.) of actinide species in a natural environment but also inspire the development of efficient media, agents, or processes to capture actinides or separate heavy f-elements. Porous materials, for instance, are capable of extracting, capturing, and immobilizing radionuclides through confinement and adsorption,[69−71] which were found to be thermodynamically favorable.[41] Thus, there are tremendous opportunities in future research and high demands on new knowledge of how radionuclides interact with structural pores or channels of different dimensions via gas or liquid phases from both structural and thermodynamic perspectives.

AUTHOR INFORMATION

Corresponding Authors

*E-mail: hxu@lanl.gov.
*E-mail: x.guo@wsu.edu.
*E-mail: d.wu@wsu.edu.

ORCID

Hui Sun: 0000-0002-8544-756X
Di Wu: 0000-0001-6879-321X

Notes

The authors declare no competing financial interest.

Biographies

Gengnan Li received her B.E. from Zhejiang Sci-Tech University, China, in 2012. She earned her Ph.D. in Materials Science and Engineering from East China University of Science and Technology, China, in 2017. She is currently a Postdoctoral Research Fellow under the guidance of Professor Di Wu in the Alexandra Navrotsky Institute for Experimental Thermodynamics and the Gene and Linda Voiland School of Chemical Engineering and Bioengineering at Washington State University. Her research interests encompass synthesis, characterization, and experimental thermodynamic (calorimetric) studies on catalytic and electrochemical materials.

Hui Sun is an Associate Professor in the State Key Laboratory of Chemical Engineering and Petroleum Processing Research Center at East China University of Science and Technology (ECUST), China. He received his B.S. in 2004 from Jiangnan University and Ph.D. from ECUST in 2009. He worked in the Peter A. Rock Thermochemistry Laboratory and NEAT ORU at the University of California, Davis, as a visiting scholar from 2013 to 2014. His research focuses on zeolites, adsorption, separation and purification, catalysis, and petroleum engineering.

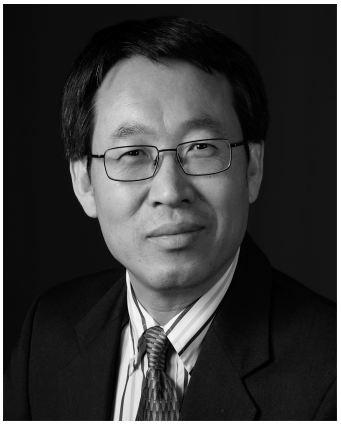

Hongwu Xu is a Senior Scientist at the Earth and Environmental Sciences Division of Los Alamos National Laboratory. He received his Ph.D. and M.A. in Geosciences from Princeton University and his M.S. and B.S. in Crystallography, Mineralogy, Petrology and Geochemistry from Nanjing University. His research interests focus on determination of structure−stability relationships of both natural minerals and synthetic materials at high-pressure variable-temperature conditions using synchrotron X-ray/neutron scattering and calorimetric techniques.

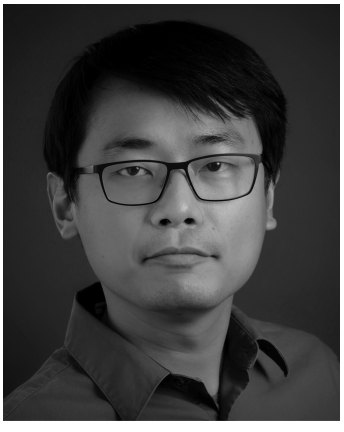

DOI: 10.1021/acs.jpcc.7b07450
J. Phys. Chem. C 2017, 121, 26141−26154

Xiaofeng Guo is an Assistant Professor in the Department of Chemistry and the Alexandra Navrotsky Institute for Experimental Thermodynamics at Washington State University. He received his Ph.D. in Chemistry from the University of California, Davis, in 2014 and was a G. T. Seaborg Postdoctoral fellow at Los Alamos National Laboratory (2015−2017). His current research interests are thermodynamics of lanthanides, actinide-containing phases, nuclear fuels and wastes, nanosized materials in the nuclear technology application, and behaviors of minerals and materials under high-temperature, high-pressure, and hydrothermal conditions.

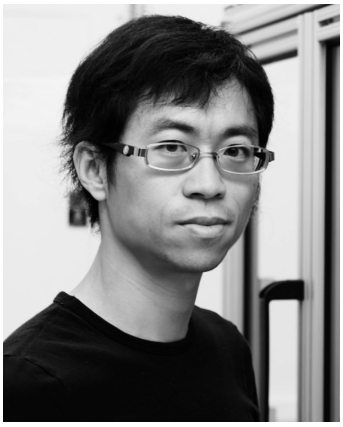

Di Wu is an Assistant Professor in the Gene and Linda Voiland School of Chemical Engineering and Bioengineering at Washington State University (WSU). He is also the founding Director of the Alexandra Navrotsky Institute for Experimental Thermodynamics (AlexInstitute) and an affiliate faculty member in the Department of Chemistry, Materials Science & Engineering Program and the Institute for Nuclear Science and Technology at WSU. He earned his B.S. from Zhejiang University, China, in 2006, M.S. from the University of Akron in 2008, and Ph.D. from the University of California, Davis under the guidance of Professor Alexandra Navrotsky, in 2012, all in Chemical Engineering. He was a postdoctoral fellow at the Peter A. Rock Thermochemistry Laboratory and NEAT ORU at the University of California, Davis, from 2013 to 2016. His research interests include physics and chemistry of material surfaces, catalysis, porous material synthesis, electrochemical materials, thermodynamics, calorimetry, nanogeoscience, and nanotechnology.

■ ACKNOWLEDGMENTS

We sincerely thank Prof. Alexandra Navrotsky at University of California, Davis, for the inspiration, guidance, and generous support. We are also grateful to Dr. Renqin Zhang for his invaluable contributions and discussions and Dr. Yushen Han and his colleagues for their amazing graphics and cover art. We also thank Jiyuan Zhong for his high quality biographical photography. H.S. thanks the National Natural Science Foundation of China for financial support under the Training Program of the Major Research Plan (Grant 91634112) and the Natural Science Foundation of Shanghai for financial support under the Natural Science Fund for Young Scholar (Grant 16ZR1408100). This work was supported by the institutional funds from the Gene and Linda Voiland School of Chemical Engineering and Bioengineering at Washington State University.

■ REFERENCES

(1) Xiao, D. J.; Bloch, E. D.; Mason, J. A.; Queen, W. L.; Hudson, M. R.; Planas, N.; Borycz, J.; Dzubak, A. L.; Verma, P.; Lee, K.; et al. Oxidation of Ethane to Ethanol by N_2O in a Metal-Organic Framework with Coordinatively Unsaturated Iron (II) Sites. *Nat. Chem.* **2014**, *6*, 590−595.

(2) Sun, J.; Baylon, R. A. L.; Liu, C.; Mei, D.; Martin, K.; Venkitasubramanian, P.; Wang, Y. Key Roles of Lewis Acid-Base Pairs on $Zn_xZr_yO_z$ in Direct Ethanol/Acetone to Isobutene Conversion. *J. Am. Chem. Soc.* **2016**, *138*, 507−517.

(3) Luo, F.; Yan, C.; Dang, L.; Krishna, R.; Zhou, W.; Wu, H.; Dong, X.; Han, Y.; Hu, T.; O'Keffe, M.; et al. UTSA-74: A MOF-74 Isomer with Two Accessible Binding Sites Per Metal Center for Highly Selective Gas Separation. *J. Am. Chem. Soc.* **2016**, *138*, 5678−5684.

(4) Hartlieb, K. J.; Holcroft, J. M.; Moghadam, P. Z.; Vermeulen, N. A.; Algaradah, M. M.; Nassar, M. S.; Botros, Y. Y.; Snurr, R. Q.; Stoddart, J. F. CD-MOF: A Versatile Separation Medium. *J. Am. Chem. Soc.* **2016**, *138*, 2292−2301.

(5) Herm, Z. R.; Bloch, E. D.; Long, J. R. Hydrocarbon Separations in Metal-Organic Frameworks. *Chem. Mater.* **2014**, *26*, 323−338.

(6) Zones, S. I.; Nakagawa, Y.; Yuen, L. T.; Harris, T. V. Guest/Host Interactions in High Silica Zeolite Synthesis: $[5.2.1.0^{2,6}]$-Tricyclodecanes as Template Molecule. *J. Am. Chem. Soc.* **1996**, *118*, 7558−7567.

(7) Wagner, P.; Nakagawa, Y.; Lee, G. S.; Davis, M. E.; Elomari, S.; Medrud, R. C.; Zones, S. I. Guest/Host Relationships in the Synthesis of the Novel Cage-Based Zeolites SSZ-35, SSZ-36, and SSZ-39. *J. Am. Chem. Soc.* **2000**, *122*, 263−273.

(8) Lee, H.; Dellatore, S. M.; Miller, W. M.; Messersmith, P. B. Mussel-Inspired Surface Chemistry for Multifunctional Coatings. *Science* **2007**, *318*, 426−430.

(9) Chen, Y.; Xianyu, Y.; Jiang, X. Surface Modification of Gold Nanoparticles with Small Molecules for Biochemical Analysis. *Acc. Chem. Res.* **2017**, *50*, 310−319.

(10) Sun, Y. M.; Fang, H. Y.; Pan, L. J.; Han, M.; Xu, S.; Wane, X. W.; Xu, B.; Wu, Y. Impact of Surface-Bound Small Molecules on the Thermoelectric Property of Self-Assembled Ag_2Te Nanocrystal Thin Films. *Nano Lett.* **2015**, *15*, 3748−3756.

(11) Brusseau, M. L.; Kookana, R. S.; Oliver, D. P.; Rogers, S.; McLaughlin, M. J. Transport and Fate of Organic Contaminants in the Subsurface. *Contaminants and the Soil Environment in the Australasia-Pacific Region* **1996**, 95−124.

(12) Sabatini, D. A.; Knox, R. C. Transport and Remediation of Subsurface Contaminants - Review and Future-Directions. *ACS. Sym. Ser.* **1992**, *491*, 234−240.

(13) Ratner, B. D. *Biomaterials Science: An Introduction to Materials in Medicine*, 3rd ed.; Elsevier/Academic Press: Amsterdam, The Netherlands, Boston, MA, 2013; pp 1519.

(14) Horcajada, P.; Chalati, T.; Serre, C.; Gillet, B.; Sebrie, C.; Baati, T.; Eubank, J. F.; Heurtaux, D.; Clayette, P.; Kreuz, C.; et al. Porous Metal-Organic Framework Nanoscale Carriers as a Potential Platform for Drug Delivery and Imaging. *Nat. Mater.* **2010**, *9*, 172−178.

(15) Anglin, E. J.; Cheng, L. Y.; Freeman, W. R.; Sailor, M. J. Porous Silicon in Drug Delivery Devices and Materials. *Adv. Drug Delivery Rev.* **2008**, *60*, 1266−1277.

(16) Navrotsky, A. Progress and New Directions in Calorimetry: A 2014 Perspective. *J. Am. Ceram. Soc.* **2014**, *97*, 3349−3359.

(17) Navrotsky, A.; Trofymluk, O.; Levchenko, A. A. Thermochemistry of Microporous and Mesoporous Materials. *Chem. Rev.* **2009**, *109*, 3885−3902.

(18) Wu, D.; Navrotsky, A. Thermodynamics of Metal-Organic Frameworks. *J. Solid State Chem.* **2015**, *223*, 53−58.

(19) Yang, S. Y.; Navrotsky, A. Energetics of Formation and Hydration of Ion-Exchanged Zeolite Y. *Microporous Mesoporous Mater.* **2000**, *41*, 345−346.

(20) Piccione, P. M.; Yang, S. Y.; Navrotsky, A.; Davis, M. E. Thermodynamics of Pure-Silica Molecular Sieve Synthesis. *J. Phys. Chem. B* **2002**, *106*, 5312−5312.

(21) Piccione, P. M.; Laberty, C.; Yang, S. Y.; Camblor, M. A.; Navrotsky, A.; Davis, M. E. Thermochemistry of Pure-Silica Zeolites. *J. Phys. Chem. B* **2000**, *104*, 10001−10011.

(22) Wu, D.; McDonald, T. M.; Quan, Z.; Ushakov, S. V.; Zhang, P.; Long, J. R.; Navrotsky, A. Thermodynamic Complexity of Carbon

DOI: 10.1021/acs.jpcc.7b07450
J. Phys. Chem. C 2017, 121, 26141−26154

Capture in Alkylamine-Functionalized Metal-Organic Frameworks. *J. Mater. Chem. A* **2015**, *3*, 4248−4254.
(23) Wu, D.; Gassensmith, J. J.; Gouvea, D.; Ushakov, S.; Stoddart, J. F.; Navrotsky, A. Direct Calorimetric Measurement of Enthalpy of Adsorption of Carbon Dioxide on CD-MOF-2, a Green Metal-Organic Framework. *J. Am. Chem. Soc.* **2013**, *135*, 6790−6793.
(24) Akimbekov, Z.; Wu, D.; Brozek, C. K.; Dincă, M.; Navrotsky, A. Thermodynamics of Solvent Interaction with the Metal-Organic Framework MOF-5. *Phys. Chem. Chem. Phys.* **2016**, *18*, 1158−62.
(25) Wu, D.; Guo, X.; Sun, H.; Navrotsky, A. Thermodynamics of Methane Adsorption on Copper HKUST-1 at Low Pressure. *J. Phys. Chem. Lett.* **2015**, *6*, 2439−43.
(26) Wu, D.; Guo, X.; Sun, H.; Navrotsky, A. Interplay of Confinement and Surface Energetics in the Interaction of Water with a Metal−Organic Framework. *J. Phys. Chem. C* **2016**, *120*, 7562−7567.
(27) Bhunia, M. K.; Hughes, J. T.; Fettinger, J. C.; Navrotsky, A. Thermochemistry of Paddle Wheel MOFs: Cu-HKUST-1 and Zn-HKUST-1. *Langmuir* **2013**, *29*, 8140−8145.
(28) Sun, H.; Wu, D.; Guo, X.; Shen, B.; Liu, J.; Navrotsky, A. Energetics of Confinement of *n*-Hexane in Ca-Na Ion Exchanged Zeolite A. *J. Phys. Chem. C* **2014**, *118*, 25590−25596.
(29) Sun, H.; Wu, D.; Guo, X.; Shen, B.; Navrotsky, A. Energetics of Sodium-Calcium Exchanged Zeolite A. *Phys. Chem. Chem. Phys.* **2015**, *17*, 11198−11203.
(30) Sun, H.; Wu, D.; Liu, K.; Guo, X.; Navrotsky, A. Energetics of Alkali and Alkaline Earth Ion−Exchanged Zeolite A. *J. Phys. Chem. C* **2016**, *120*, 15251−15256.
(31) Christensen, H.; Sunder, S. Current State of Knowledge of Water Radiolysis Effects on Spent Nuclear Fuel Corrosion. *Nucl. Technol.* **2000**, *131*, 102−123.
(32) Wu, D.; Hwang, S. J.; Zones, S. I.; Navrotsky, A. Guest−Host Interactions of a Rigid Organic Molecule in Porous Silica Frameworks. *Proc. Natl. Acad. Sci. U. S. A.* **2014**, *111*, 1720−1725.
(33) Wu, D.; Navrotsky, A. Small Molecule − Silica Interactions in Porous Silica Structures. *Geochim. Cosmochim. Acta* **2013**, *109*, 38−50.
(34) Wu, D.; Navrotsky, A. Probing the Energetics of Organic-Nanoparticle Interactions of Ethanol on Calcite. *Proc. Natl. Acad. Sci. U. S. A.* **2015**, *112*, 5314−5318.
(35) Liu, N. W.; Guo, X. F.; Navrotsky, A.; Shi, L.; Wu, D. Thermodynamic Complexity of Sulfated Zirconia Catalysts. *J. Catal.* **2016**, *342*, 158−163.
(36) Sarge, S. M.; Hohne, G. W. H.; Hemminger, W. Calorimetry: Fundamentals, Instrumentation and Applications. *Calorimetry: Fundamentals, Instrumentation and Applications* **2014**, 1−280.
(37) Ushakov, S. V.; Navrotsky, A. Direct Measurements of Water Adsorption Enthalpy on Hafnia and Zirconia. *Appl. Phys. Lett.* **2005**, *87*, 164103.
(38) Navrotsky, A. Progress and New Directions in High Temperature Calorimetry Revisited. *Phys. Chem. Miner.* **1997**, *24*, 222−241.
(39) Hughes, J. T.; Bennett, T. D.; Cheetham, A. K.; Navrotsky, A. Thermochemistry of Zeolitic Imidazolate Frameworks of Varying Porosity. *J. Am. Chem. Soc.* **2013**, *135*, 598−601.
(40) Hughes, J. T.; Navrotsky, A. MOF-5: Enthalpy of Formation and Energy Landscape of Porous Materials. *J. Am. Chem. Soc.* **2011**, *133*, 9184−9187.
(41) Hughes, J. T.; Sava, D. F.; Nenoff, T. M.; Navrotsky, A. Thermochemical Evidence for Strong Iodine Chemisorption by ZIF-8. *J. Am. Chem. Soc.* **2013**, *135*, 16256−16259.
(42) Silvestre-Albero, J.; de Salazar, C. G.; Sepulveda-Escribano, A.; Rodriguez-Reinoso, F. Characterization of Microporous Solids by Immersion Calorimetry. *Colloids Surf., A* **2001**, *187*−*188*, 151−165.
(43) Furukawa, H.; Cordova, K. E.; O'Keeffe, M.; Yaghi, O. M. The Chemistry and Applications of Metal-Organic Frameworks. *Science* **2013**, *341*, 1230444.
(44) Smaldone, R. A.; Forgan, R. S.; Furukawa, H.; Gassensmith, J. J.; Slawin, A. M. Z.; Yaghi, O. M.; Stoddart, J. F. Metal-Organic Frameworks from Edible Natural Products. *Angew. Chem., Int. Ed.* **2010**, *49*, 8630−8634.
(45) Gassensmith, J. J.; Furukawa, H.; Smaldone, R. A.; Forgan, R. S.; Botros, Y. Y.; Yaghi, O. M.; Stoddart, J. F. Strong and Reversible Binding of Carbon Dioxide in a Green Metal-Organic Framework. *J. Am. Chem. Soc.* **2011**, *133*, 15312−153155.
(46) McDonald, T. M.; Mason, J. A.; Kong, X.; Bloch, E. D.; Gygi, D.; Dani, A.; Crocellà, V.; Glordanino, F.; Odoh, S. O.; Drisdell, W. S.; et al. Cooperative Insertion of CO_2 in Diamine-Appended Metal-Organic Frameworks. *Nature* **2015**, *519*, 303−308.
(47) Hulvey, Z.; Vlaisavljevich, B.; Mason, J. A.; Tsivion, E.; Dougherty, T. P.; Bloch, E. D.; Head-Gordon, M.; Smit, B.; Long, J. R.; Brown, C. M. Critical Factors Driving the High Volumetric Uptake of Methane in $Cu_3(btc)_2$. *J. Am. Chem. Soc.* **2015**, *137*, 10816−10825.
(48) Brozek, C. K.; Michaelis, V. K.; Ong, T. C.; Bellarosa, L.; Lopez, N.; Griffin, R. G.; Dincă, M. Dynamic DMF Binding in MOF-5 Enables the Formation of Metastable Cobalt-Substituted MOF-5 Analogues. *ACS Cent. Sci.* **2015**, *1*, 252−260.
(49) Wu, D.; Guo, X. F.; Sun, H.; Navrotsky, A. Energy Landscape of Water and Ethanol on Silica Surfaces. *J. Phys. Chem. C* **2015**, *119*, 15428−15433.
(50) Sand, K. K.; Yang, M.; Makovicky, E.; Cooke, D. J.; Hassenkam, T.; Bechgaard, K.; Stipp, S. L. Binding of Ethanol on Calcite: The Role of the OH Bond and Its Relevance to Biomineralization. *Langmuir* **2010**, *26*, 15239−47.
(51) Fu, L. J.; Yang, H. M.; Hu, Y. H.; Wu, D.; Navrotsky, A. Tailoring Mesoporous Gamma-Al_2O_3 Properties by Transition Metal Doping: A Combined Experimental and Computational Study. *Chem. Mater.* **2017**, *29*, 1338−1349.
(52) Eriksen, T. E.; Eklund, U. B.; Werme, L.; Bruno, J. Dissolution of Irradiated Fuel: A Radiolytic Mass Balance Study. *J. Nucl. Mater.* **1995**, *227*, 76−82.
(53) Wronkiewicz, D. J.; Bates, J. K.; Wolf, S. F.; Buck, E. C. Ten-Year Results from Unsaturated Drip Tests with UO_2 at 90 °C: Implications for the Corrosion of Spent Nuclear Fuel. *J. Nucl. Mater.* **1996**, *238*, 78−95.
(54) Sunder, S.; Shoesmith, D. W.; Miller, N. H. Oxidation and Dissolution of Nuclear Fuel (UO_2) by the Products of the Alpha Radiolysis of Water. *J. Nucl. Mater.* **1997**, *244*, 66−74.
(55) Haschke, J. M.; Allen, T. H.; Morales, L. A. Reaction of Plutonium Dioxide with Water: Formation and Properties of PuO_{2+X}. *Science* **2000**, *287*, 285−287.
(56) Haschke, J. M.; Allen, T. H.; Morales, L. A. Surface and Corrosion Chemistry of Plutonium. *Los Alamos Sci.* **2000**, *26*, 252−273.
(57) Skomurski, F. N.; Shuller, L. C.; Ewing, R. C.; Becker, U. Corrosion of UO_2 and ThO_2: A Quantum-Mechanical Investigation. *J. Nucl. Mater.* **2008**, *375*, 290−310.
(58) Haire, R. G.; Haschke, J. M. Plutonium Oxide Systems and Related Corrosion Products. *MRS Bull.* **2001**, *26*, 689−696.
(59) Weck, P. F.; Kim, E.; Jove-Colon, C. F.; Sassani, D. C. First-Principles Study of Anhydrite, Polyhalite and Carnallite. *Chem. Phys. Lett.* **2014**, *594*, 1−5.
(60) Stewart, F. H. *Marine Evaporite*; US Geological Survey Professional Paper 440-Y, 1963.
(61) Guo, X.; Szenknect, S.; Mesbah, A.; Labs, S.; Clavier, N.; Poinssot, C.; Ushakov, S.; Curtius, H.; Bosbach, D.; Ewing, R. C.; et al. Thermodynamics of Formation of Coffinite, $USiO_4$. *Proc. Natl. Acad. Sci. U. S. A.* **2015**, *112*, 6551−6555.
(62) Kubatko, K. A. H.; Helean, K. B.; Navrotsky, A.; Burns, P. C. Stability of Peroxide-Containing Uranyl Minerals. *Science* **2003**, *302*, 1191−1193.
(63) McNamara, B.; Buck, E.; Hanson, B. Observation of Studtite and Metastudtite on Spent Fuel. *Mater. Res. Soc. Symp. Proc.* **2003**, *757*, 401−406.
(64) Hanson, B.; McNamara, B.; Buck, E.; Friese, J.; Jenson, E.; Krupka, K.; Arey, B. Corrosion of Commercial Spent Nuclear Fuel. 1. Formation of Studtite and Metastudtite. *Radiochim. Acta* **2005**, *93*, 159−168.

DOI: 10.1021/acs.jpcc.7b07450
J. Phys. Chem. C 2017, 121, 26141−26154

(65) Guo, X.; Ushakov, S. V.; Labs, S.; Curtius, H.; Bosbach, D.; Navrotsky, A. Energetics of Metastudtite and Implications for Nuclear Waste Alteration. *Proc. Natl. Acad. Sci. U. S. A.* **2014**, *111*, 17737−17742.
(66) Soderholm, L.; Almond, P. M.; Skanthakumar, S.; Wilson, R. E.; Burns, P. C. The Structure of the Plutonium Oxide Nanocluster $[Pu_{38}O_{56}Cl_{54}(H_2O)_8]^{14-}$. *Angew. Chem., Int. Ed.* **2008**, *47*, 298−302.
(67) Armstrong, C. R.; Nyman, M.; Shvareva, T.; Sigmon, G. E.; Burns, P. C.; Navrotsky, A. Uranyl Peroxide Enhanced Nuclear Fuel Corrosion in Seawater. *Proc. Natl. Acad. Sci. U. S. A.* **2012**, *109*, 1874−1877.
(68) Burns, P. C.; Ewing, R. C.; Navrotsky, A. Nuclear Fuel in a Reactor Accident. *Science* **2012**, *335*, 1184−1188.
(69) Sava, D. F.; Garino, T. J.; Nenoff, T. M. Iodine Confinement into Metal-Organic Frameworks (MOFs): Low-Temperature Sintering Glasses to Form Novel Glass Composite Material (GCM) Alternative Waste Forms. *Ind. Eng. Chem. Res.* **2012**, *51*, 614−620.
(70) Banerjee, D.; Xu, W.; Nie, Z.; Johnson, L. E. V.; Coghlan, C.; Sushko, M. L.; Kim, D.; Schweiger, M. J.; Kruger, A. A.; Doonan, C. J.; et al. Zirconium-Based Metal-Organic Framework for Removal of Perrhenate from Water. *Inorg. Chem.* **2016**, *55*, 8241−8243.
(71) Demir, S.; Brune, N. K.; Humbeck, J. F. V.; Mason, J. A.; Plakhova, T. V.; Wang, S.; Tian, G.; Minasian, S. G.; Tyliszczak, T.; Yaita, T.; et al. Extraction of Lanthanide and Actinide Ions from Aqueous Mixtures Using a Carboxylic Acid-Functionalized Porous Aromatic Framework. *ACS Cent. Sci.* **2016**, *2*, 253−265.

DOI: 10.1021/acs.jpcc.7b07450
J. Phys. Chem. C 2017, 121, 26141−26154